

A Selenium-Containing Diarylamido Pincer Ligand: Synthesis and Coordination Chemistry with Group 10 Metals

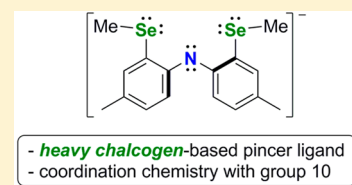
Bronte J. Charette and Jamie S. Ritchh*

Department of Chemistry, The University of Winnipeg, 515 Portage Avenue, Winnipeg, Manitoba R3J 2N6, Canada

Department of Chemistry, University of Manitoba, 360 Parker Building, Winnipeg, Manitoba R3T 2N2, Canada

S Supporting Information

ABSTRACT: The synthesis of new bifunctional organoselenium diarylamine compounds $\text{RN}(4\text{-Me-2-SeMe-C}_6\text{H}_3)_2$ ($\text{R} = \text{Me}$: **1**; $\text{R} = \textit{tert}$ -butoxycarbonyl (Boc): **2**; $\text{R} = \text{H}$: **3-H**) via aryllithium chemistry is disclosed. Compound **1** serves as a *Se,Se*-bidentate neutral ligand toward Pd^{II} , forming the coordination complex $\{\text{PdCl}_2[\text{MeN}(4\text{-Me-2-SeMe-C}_6\text{H}_3)_2\text{-}\kappa^2\text{Se}]\}$ (**1-Pd**) in reaction with $[\text{PdCl}_2(\text{COD})]$ ($\text{COD} = 1,5\text{-cyclooctadiene}$), while the protio ligand **3-H** forms tridentate pincer complexes $[\text{MCl}(\text{N}(4\text{-Me-2-SeMe-C}_6\text{H}_3)_2)]$ ($\text{M} = \text{Pd}$: **3-Pd**; $\text{M} = \text{Pt}$: **3-Pt**) with $[\text{MCl}_2(\text{COD})]$ ($\text{M} = \text{Pd, Pt}$) in the presence of triethylamine. Complex **1-Pd** does not undergo *N-C* cleavage at high temperature, unlike related alkylphosphine-bearing complexes. All compounds have been characterized by multinuclear (^1H , ^{13}C , ^{77}Se) NMR spectroscopy, and crystal structures of **1**, **1-Pd**, **3-Pd**, and **3-Pt** are reported. Additionally, density functional theory calculations have been performed on the pincer complexes to contrast them with well-known analogues containing phosphine donor groups.



INTRODUCTION

Pincer ligands, which feature three Lewis base donors in a planar arrangement, have enjoyed popularity in the coordination chemistry of transition metals since their discovery in the 1970s.¹ The rigid tridentate framework can confer thermal stability and solubility to metal complexes, while offering electronic and steric tunability via the donor heteroatoms and organic substitution. Well-studied arrangements include monoanionic PCP and PNP ligands, though many others are reported. In addition to their illuminating fundamental coordination chemistry, practical applications of pincer ligand complexes have been found. For instance, some catalytic transformations are promoted by pincer complexes: polymerization of alkenes and alkynes,^{2,3} hydrosilylation,^{4,5} decarbonylation of ethanol to methane,⁶ and dehydrogenation.^{7,8}

Phosphorus and nitrogen are perhaps the most commonly employed heteroatom donors on the “arms” of a pincer ligand. Sulfur-bearing pincers have been known since 1980, when Shaw and co-workers reported that 1,3-di-*tert*-butylthiobenzene undergoes C–H metalation with Na_2PdCl_4 to form a LPdCl complex.⁹ Recently, however, investigations into sulfur- and selenium-containing pincers have intensified and provided examples of unique bonding and reactivity. The sulfur-substituted diarylamido ligand $[\text{N}(2\text{-}^t\text{Bu-C}_6\text{H}_4)_2]^-$ was reported by Peters and co-workers in 2004, who found it able to stabilize a redox-active Cu^{I} dimer and facilitate reversible conversion to a $\text{Cu}^{1.5}/\text{Cu}^{1.5}$ state.¹⁰ Other SNS ligands have been used to generate the catalysts $[\text{CrCl}(\text{N}(\text{SiMe}_2\text{CH}_2\text{SR})_2)_2]$ ($\text{R} = \text{Cy, Ph, } ^t\text{Bu}$)¹¹ and $[\text{RuCl}_2(\text{PPh}_3)(\text{HN}(\text{CH}_2\text{CH}_2\text{SEt})_2)]$,¹² for ethane oligomerization and ester hydrogenation, respectively. A chiral bis(sulfoxide) $[(\text{SO})\text{N}(\text{SO})]^-$ ligand has been reported by Dorta and co-workers,¹³ which was coordinated to Rh^{I} and Rh^{III} , and underwent partial stereoselective reduction to a $[(\text{SO})\text{NS}]^-$ ligand upon reaction with $[\text{RhCl}(\text{COE})]_2$.

Some examples of selenium-containing SeXSe pincer ligands ($\text{X} = \text{C, N}$) are shown in Figure 1. Yao and co-workers reported

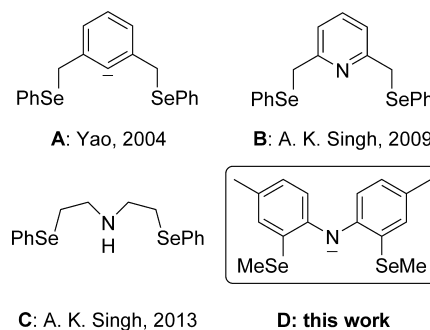


Figure 1. Selected examples of selenium-containing pincer ligands.

the $[\text{SeCSe}]^-$ ligand **A** in 2004,¹⁴ which yielded a palladium(II) complex with quite high activity for the Heck reaction—the catalyst $[\text{PdCl}(\text{A})]$ and the protio ligand **HA** are now commercially available. The neutral SeNSe ligands **B**¹⁵ and **C**¹⁶ also yield palladium(II) complexes that promote the Heck coupling of alkenes and aryl halides. The catalytic properties of selenium-containing pincer ligands have been reviewed,¹⁷ and these systems seem poised to achieve further applications as their chemistry is explored in more depth. In some reactions, the complexes appear to act as precatalysts for the formation of catalytically active Pd_xSe_y nanoparticles, rather than single sites for homogeneous catalysis.¹⁸ Nonetheless, the scope of these ligands has not been explored to the same extent as is the case

Received: May 16, 2016

for more common phosphorus or nitrogen analogues, and it would prove informative to develop a more varied library of selenium-containing pincers to study structure–activity relationships.

Taking interest in this burgeoning area of research, we noted that no examples of anionic $[\text{SeNSe}]^-$ systems have been reported, and thus we sought to prepare one in order to expand the library of known Se-containing pincer ligands. The diarylamido backbone is flexible (unlike a carbazole-type framework) yet chemically stable and has been successfully incorporated into, for example, $[\text{SNS}]^-$ and $[\text{PNP}]^-$ ligands.^{10,19} To obtain complexes amenable to NMR analysis, we focused our preliminary coordination chemistry efforts on diamagnetic metal ions. This contribution highlights the synthesis of the first heavy donor atom pincer ligand of type **D** and its coordination chemistry with group 10 M^{2+} ions.

EXPERIMENTAL SECTION

General Procedures. Unless specified otherwise, all manipulations were performed under an argon atmosphere using standard Schlenk line or glovebox techniques. Diethyl ether and THF were treated with Na/benzophenone, vacuum distilled, and sparged with argon. Toluene, hexanes, and dichloromethane were dried by passage through two columns of activated alumina and sparged with argon. C_6D_6 and d_8 -THF were dried with Na/benzophenone, while CDCl_3 was dried over CaH_2 ; deuterated solvents were degassed using at least three freeze–pump–thaw cycles. All solvents were stored over 4 Å molecular sieves in PTFE-sealed glass vessels.

The reagents $\text{HN}(\text{C}_7\text{H}_6\text{Br})_2$,²⁰ $[\text{NaN}(\text{SiMe}_3)_2]$,²¹ $[\text{PdCl}_2(\text{COD})]$,²² $[\text{PtCl}_2(\text{COD})]$,²³ and $[\text{NiCl}_2(\text{DME})]$ ²⁴ (DME = 1,2-dimethoxyethane) were prepared according to literature procedures. Iodomethane, Boc_2O , 1.6 M *n*-butyllithium in hexanes, dimethyl diselenide, trifluoroacetic acid, triethylamine, 4-dimethylaminopyridine, $[\text{Ag}(\text{OTf})]$, $[\text{NiCl}_2]$, $[\text{NiCl}_2(\text{H}_2\text{O})_6]$, $[\text{NiBr}_2]$, $[\text{Ni}(\text{OTf})_2]$ (OTf = trifluoromethanesulfonate), $[\text{Ir}_2(\text{C}_8\text{H}_{14})_4\text{Cl}_2]$, and $[\text{Rh}_2(\text{C}_8\text{H}_{14})_4\text{Cl}_2]$ were purchased from commercial sources and used as received.

Instrumentation. NMR spectra were collected on a Bruker 400 MHz Avance III spectrometer. Chemical shifts are reported in parts per million (ppm). ^1H and ^{13}C resonances are referenced to residual CHCl_3 (δ 7.26) and CDCl_3 (δ 77.27), respectively, in the deuterated solvent. ^{77}Se NMR spectra were referenced externally using Pb_2Se_2 in CDCl_3 at δ 463 ppm. Elemental analyses were performed by Canadian Microanalytical Ltd. (Delta, BC, Canada). High resolution mass spectra (HRMS) were obtained using an orthogonal time-of-flight mass spectrometer with electrospray ionization (ESI).

$[\text{NaN}(\text{C}_7\text{H}_6\text{Br})_2]$. $[\text{NaN}(\text{SiMe}_3)_2]$ (0.272 g, 1.48 mmol) in toluene (10 mL) was added via cannula to a solution of $\text{HN}(\text{C}_7\text{H}_6\text{Br})_2$ (0.503 g, 1.41 mmol) in toluene (10 mL). The resulting yellow solution was stirred at room temperature for 4 h. The volatiles were removed *in vacuo* to afford a light yellow solid (0.442 g, 86.3%). ^1H NMR (d_8 -THF, 400 MHz): δ 7.08 (s, 2H, Ar–H), 6.77 (d, 2H, J = 8.0 Hz, Ar–H), 6.60 (d, 2H, J = 8.4 Hz, Ar–H), 2.09 (s, 6H, Ar– CH_3). $^{13}\text{C}\{^1\text{H}\}$ NMR (d_8 -THF, 100 MHz): δ 133.2 (Ar–C), 132.6 (Ar–C), 132.4 (Ar–C), 132.0 (Ar–C), 128.3 (Ar–C), 118.7 (Ar–C), 19.2 (Ar– CH_3).

N-Methyl-bis(2-bromo-4-methylphenyl)amine. *N*-methyl-bis(2-bromo-4-methylphenyl)amine was prepared by a modified literature procedure.²⁵ Iodomethane (0.190 mL, 3.0 mmol) was added to a solution of $[\text{NaN}(\text{C}_7\text{H}_6\text{Br})_2]$ (0.754 g, 2.0 mmol) in THF (30 mL). The reaction mixture was stirred at room temperature overnight. The volatiles were removed *in vacuo*; the residue was washed with a 30% EtOH/ H_2O mixture then dried at 60 °C for 1 h. The light yellow solid was dissolved in diethyl ether and passed over a plug of silica. The volatiles were removed *in vacuo* to afford a yellow solid (0.523 g, 70.9%). ^1H NMR (CDCl_3 , 400 MHz): δ 7.38 (s, 2H, Ar–H), 7.03 (d, 2H, J = 8.0 Hz, Ar–H), 6.87 (d, 2H, J = 8.0 Hz, Ar–H), 3.17 (s, 3H, N– CH_3), 2.28 (s, 6H, Ar– CH_3).

$(\text{C}_7\text{H}_6\text{SeMe})_2\text{NMe}$ (**1**). *n*-BuLi (1.63 mL of 1.33 M solution in hexanes, 2.17 mmol) was added dropwise to a solution of $\text{MeN}(\text{C}_7\text{H}_6\text{Br})_2$ (0.397 g, 1.0 mmol) in diethyl ether (15 mL) at -78 °C. The yellow solution was warmed to room temperature and stirred for 30 min, then cooled to -78 °C. At this point, Me_2Se_2 (0.202 mL, 2.14 mmol) was added dropwise. The mixture became heterogeneous immediately and was stirred overnight at room temperature. The reaction mixture was quenched with water (30 mL) and CH_2Cl_2 (40 mL). The aqueous layers were extracted with additional CH_2Cl_2 (2 \times 20 mL). The combined organic layers were washed with brine and dried over Na_2SO_4 before the solvent was removed *in vacuo*. The resulting white solid was recrystallized in Et_2O at -35 °C to afford clear crystals (0.099 g, 24.8%, mp 118–120 °C). ^1H NMR (CDCl_3 , 400 MHz): δ 7.03 (s, 2H, Ar–H), 6.92 (d, 2H, J = 8.0 Hz, Ar–H), 6.83 (d, 2H, J = 8.0 Hz, Ar–H), 3.17 (s, 3H, N– CH_3), 2.32 (s, 6H, Ar– CH_3), 2.24 (s, 6H, $^2J_{\text{H-Se}} = 12$ Hz, Se– CH_3). $^{13}\text{C}\{^1\text{H}\}$ NMR (CDCl_3 , 100 MHz): δ 146.8 (Ar–C), 133.82 (Ar–C), 130.0 (Ar–C), 129.0 (Ar–C), 126.6 (Ar–C), 122.1 (Ar–C), 41.6 (N– CH_3), 20.9 (Ar– CH_3), 5.9 (Se– CH_3). $^{77}\text{Se}\{^1\text{H}\}$ NMR (CDCl_3 , 76 MHz): δ 178. Anal. calcd. (%) for $\text{C}_{17}\text{H}_{21}\text{NSe}_2$ (397.28): C, 51.40; H, 5.33; N, 3.53. Found: C, 51.43; H, 5.34; N, 3.52.

$[(\text{Se}^{\text{Me}}\text{Se})\text{PdCl}_2]$ (**1-Pd**). $[\text{PdCl}_2(\text{COD})]$ (0.039 g, 0.136 mmol) and **1** (0.055 g, 0.139 mmol) were added to a Schlenk flask with toluene (2 mL). The reaction mixture was stirred at 100 °C for 2 h; then the solvent was removed *in vacuo* to afford an orange powder (0.046 g, 57.8%, mp 216–221 °C dec). Recrystallization from CH_2Cl_2 and Et_2O was performed prior to elemental analysis; carbon percentages were consistently low, possibly due to incomplete combustion. ^1H NMR (CDCl_3 , 400 MHz): δ 7.23 (d, 2H, J = 8.0 Hz, Ar–H), 7.04 (d, 2H, J = 8.0 Hz, Ar–H), 7.01 (s, 2H, Ar–H), 3.18 (s, 3H, N– CH_3), 2.69 (s, 6H, $^2J_{\text{H-Se}} = 12$ Hz, Se– CH_3), 2.41 (s, 3H, Ar– CH_3). $^{13}\text{C}\{^1\text{H}\}$ NMR (CDCl_3 , 100 MHz): δ 145.5 (Ar–C), 136.7 (Ar–C), 131.4 (Ar–C), 128.2 (Ar–C), 124.3 (Ar–C), 123.0 (Ar–C), 43.6 (N– CH_3), 21.1 (Ar– CH_3), 12.8 (Se– CH_3). $^{77}\text{Se}\{^1\text{H}\}$ NMR (CDCl_3 , 76 MHz): δ 278. Anal. calcd. (%) for $\text{C}_{17}\text{H}_{21}\text{NCl}_2\text{PdSe}_2$ (574.60): C, 35.53; H, 3.68; N, 2.44. Found: C, 34.06; H, 3.26; N, 2.21.

$(\text{C}_7\text{H}_6\text{Br})_2\text{NBoc}$. The reagent $[\text{NaN}(\text{C}_7\text{H}_6\text{Br})_2]$ (0.418 g, 1.18 mmol) was dissolved in THF (20 mL) and stirred at room temperature. Boc_2O (0.299 g, 1.37 mmol) was added dropwise to the yellow solution, and the mixture was stirred overnight. The reaction mixture was quenched with 5 drops of methanol before solvent was removed *in vacuo*. The residual oil was quenched with 1 M HCl (30 mL) and extracted with CH_2Cl_2 (3 \times 30 mL). The combined organic layers were washed with saturated NaHCO_3 (20 mL) and brine and dried with Na_2SO_4 before the solvent was removed *in vacuo* to afford a yellow solid (0.431 g, 80.3%, mp 154–157 °C). ^1H NMR (CDCl_3 , 400 MHz): δ 7.45 (d, 2H, J = 8.0 Hz, Ar–H), 7.30 (d, 2H, J = 8.0 Hz, Ar–H), 7.02 (d, 2H, J = 8.0 Hz, Ar–H), 2.31 (s, 6H, Ar– CH_3), 1.46 (s, 9H, C(CH_3)₃). $^{13}\text{C}\{^1\text{H}\}$ NMR (CDCl_3 , 100 MHz): δ 156.3 (C=O), 138.8 (Ar–C), 138.5 (Ar–C), 133.9 (Ar–C), 133.6 (Ar–C), 129.2 (Ar–C), 128.5 (Ar–C), 81.2 (C(CH_3)₃), 28.1 (C(CH_3)₃), 20.7 (Ar– CH_3). Anal. calcd. (%) for $\text{C}_{19}\text{H}_{21}\text{NBBr}_2\text{O}_2$ (455.18): C, 50.13; H, 4.65; N, 3.08. Found: C, 49.34; H, 4.64; N, 2.88.

$(\text{C}_7\text{H}_6\text{SeMe})_2\text{NBoc}$ (**2**). *n*-BuLi (9.78 mL of 1.6 M solution in hexanes, 15.6 mmol), $\text{BocN}(\text{C}_7\text{H}_6\text{Br})_2$ (3.23 g, 7.10 mmol), and Me_2Se_2 (1.2 mL, 12.68 mmol) in diethyl ether (50 mL) were reacted in a similar method to $\text{MeN}(\text{C}_7\text{H}_6\text{SeMe})_2$. The green oil was washed with cold hexanes to afford yellow crystals (0.925 g, 27.0%, mp 174–176 °C). ^1H NMR (CDCl_3 , 400 MHz): δ 7.20 (br m, 4H Ar–H), 6.89 (d, 2H, J = 8.0 Hz, Ar–H), 2.35 (s, 6H, $^2J_{\text{H-Se}} = 12$ Hz, Se– CH_3), 2.30 (br s, 6H, Ar– CH_3), 1.46 (s, 9H, C(CH_3)₃). $^{13}\text{C}\{^1\text{H}\}$ NMR (CDCl_3 , 100 MHz): δ 153.1 (C=O), 140.6 (Ar–C), 137.0 (Ar–C), 132.2 (Ar–C), 131.3 (Ar–C), 130.9 (Ar–C), 127.4 (Ar–C), 81.1 (C(CH_3)₃), 28.1 (C(CH_3)₃), 21.0 (Ar– CH_3), 7.4 (Se– CH_3). $^{77}\text{Se}\{^1\text{H}\}$ NMR (CDCl_3 , 76 MHz): δ 179, 173. Anal. calcd. (%) for $\text{C}_{21}\text{H}_{27}\text{NO}_2\text{Se}_2$ (483.36): C, 52.18; H, 5.63; N, 2.90. Found: C, 52.19; H, 5.71; N, 3.04.

$(\text{C}_7\text{H}_6\text{SeMe})_2\text{NH}$ (**3-H**). To a solution of **2** (0.925 g, 1.91 mmol) in anhydrous CH_2Cl_2 (10 mL), trifluoroacetic acid (8 mL) was added

and stirred for 1 h. The brown solution was neutralized with saturated NaHCO₃ (20 mL) and extracted with CH₂Cl₂ (3 × 20 mL). The combined organic layers were dried over MgSO₄, and solvent was removed *in vacuo* to afford a purple oil (0.701 g, 95.8%). ¹H NMR (CDCl₃, 400 MHz): δ 7.36 (s, 2H, Ar–H), 7.02 (d, 2H, *J* = 8.0 Hz, Ar–H), 6.98 (d, 2H, *J* = 8.0 Hz, Ar–H), 6.69 (br s, 1H, N–H), 2.29 (s, 6H, ²*J*_{H–Se} = 12 Hz, Se–CH₃), 2.25 (s, 6H, Ar–CH₃). ¹³C{¹H} NMR (CDCl₃, 100 MHz): δ 141.3 (Ar–C), 134.5 (Ar–C), 131.1 (Ar–C), 129.1 (Ar–C), 122.1 (Ar–C), 117.4 (Ar–C), 20.5 (Ar–CH₃), 7.7 (Se–CH₃). ⁷⁷Se{¹H} NMR (CDCl₃, 76 MHz): δ 121. HRMS-ESI (*m/z*): [M + Na]⁺ calcd. for C₁₆H₁₉NSe₂: 407.9740. Found: 407.9735.

[(SeNSe)PdCl] (3-Pd). [PdCl₂(COD)] (0.039 g, 0.137 mmol) and 3-H (0.05 g, 0.130 mmol) were added to a Schlenk flask with THF (10 mL). Triethylamine (0.035 mL, 0.251 mmol) was added, and an immediate color change from yellow to emerald green was observed. The reaction mixture was stirred at 80 °C for 1 h; then the solvent was removed *in vacuo* to afford a green powder. An analytically pure sample was obtained by recrystallization from CH₂Cl₂ and Et₂O at 0 °C as green crystals (39.7 mg, 58.0%, mp 196–200 °C dec). ¹H NMR (CDCl₃, 400 MHz): δ 7.33 (m, 2H, Ar–H), 7.08 (s, 2H, Ar–H), 6.83 (m, 2H, Ar–H), 2.74 (s, ²*J*_{H–Se} = 12 Hz, Se–CH₃, 50% isomer), 2.72 (s, ²*J*_{H–Se} = 12 Hz, Se–CH₃, 50% isomer), 2.23 (s, 6H, Ar–CH₃). ¹³C{¹H} NMR (CDCl₃, 100 MHz): δ 156.1 (Ar–C), 133.5 (Ar–C), 130.3 (Ar–C), 128.2 (Ar–C), 118.0 (Ar–C), 117.4 (Ar–C), 20.0 (Ar–CH₃), 19.1 (isomer–Se–CH₃), 18.6 (isomer–Se–CH₃). ⁷⁷Se{¹H} NMR (CDCl₃, 76 MHz): δ 306, 289. Anal. calcd. (%) for C₁₆H₁₈NCIPdSe₂ (524.11): C, 36.67; H, 3.46; N, 2.67. Found: C, 35.96; H, 3.27; N, 2.47.

[(SeNSe)PtCl] (3-Pt). [PtCl₂(COD)] (0.026 g, 0.067 mmol) and 3-H (0.025 g, 0.065 mmol) were added to a Schlenk flask with CH₂Cl₂ (2 mL). Triethylamine (0.02 mL, 0.143 mmol) was added, and an immediate color change from purple to red was observed. The reaction mixture was stirred at room temperature for 1 h; then the solvent was removed *in vacuo* to afford a red powder (35.0 mg, 87.9%, mp 240 °C dec). The compound was purified via column chromatography using CH₂Cl₂ to obtain an analytically pure sample. ¹H NMR (CDCl₃, 400 MHz): δ 7.47 (d, 2H, *J* = 8.0 Hz, Ar–H), 7.16 (s, 2H, Ar–H), 6.84 (d, 2H, *J* = 8.0 Hz, Ar–H), 2.75 (s, ²*J*_{H–Se} = 12 Hz, Se–CH₃, 66% isomer), 2.70 (s, ²*J*_{H–Se} = 12 Hz, Se–CH₃, 44% isomer), 2.28 (s, 6H, Ar–CH₃). ¹³C{¹H} NMR (CDCl₃, 100 MHz): δ 155.0 (Ar–C), 133.1 (Ar–C), 130.3 (Ar–C), 128.6 (Ar–C), 119.4 (Ar–C), 117.0 (Ar–C), 20.7 (Ar–CH₃), 20.46 (isomer–Se–CH₃), 20.0 (isomer–Se–CH₃). ⁷⁷Se{¹H} NMR (CDCl₃, 76 MHz): δ 264 (¹*J*_{Se–Pt} = 439 Hz), 253 (¹*J*_{Se–Pt} = 456 Hz). Anal. calcd. (%) for C₁₆H₁₈NCIPtSe₂ (612.77): C, 31.36; H, 2.96; N, 2.29. Found: C, 30.69; H, 2.41; N, 1.98.

General Procedure for the Attempted Synthesis of [(SeNSe)NiL]_n. 3-H and nickel(II) reagent were added to a Schlenk flask. Solvent and base were added, and the reaction mixture was stirred. Volatiles were removed *in vacuo*, and the remaining material was analyzed by ¹H NMR spectroscopy, which showed no conversion to product. Detailed reaction parameters are listed in Table S1.

Attempted Synthesis of [(SeNSe)ML]_n (M = Rh, Ir). 3-H and [M₂(C₈H₁₄)₄Cl₂] (M = Rh, Ir) were added to C₆D₆ in an NMR tube. The reaction mixture was heated to 100 °C for 2 days. NMR spectra showed a complicated mixture, and no further characterization was attempted.

X-ray Crystallography. A selected crystal of each compound was coated in oil and mounted on a polymer loop. Data were collected on a Bruker D8 Advance ECO X-ray diffractometer with Mo K α radiation (λ = 0.71073 Å) using ϕ and ω scans. Unit cells were determined from the full data set. Absorption corrections were applied either numerically via face-indexing or with multiscan methods. Using Olex2,²⁶ solutions were obtained with direct methods using the SHELXT program,²⁷ and all least-squares refinements were carried out against *F*² using SHELXL.²⁸ Non-hydrogen atoms were modeled anisotropically; hydrogen atoms were treated isotropically and placed in calculated positions using a riding model. No special considerations were necessary for the solution and refinement of the structures. Selected crystal data are presented in the Supporting Information (Table S2).

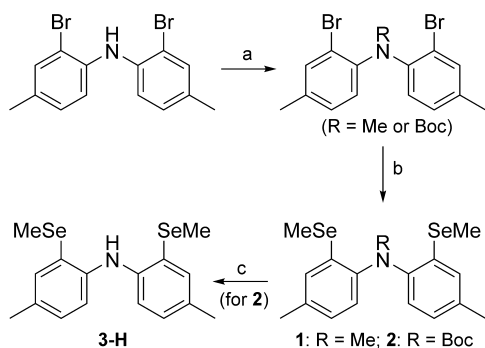
DFT Calculations. Density functional theory calculations were conducted using the software package GAMESS,²⁹ with the dispersion-corrected functional ω B97X-D,³⁰ known to provide good estimations for transition metal complex geometries.³¹ The double- ζ quality basis set def2-SVP³² was utilized for all atoms (with effective core potentials used for Pd and Pt), which includes polarization functions for both hydrogen and non-hydrogen atoms and is suitable for semiquantitative computations. Starting coordinates for gas phase, closed-shell geometry optimization of the C₂-symmetric isomers of 3-Pd and 3-Pt were garnered from the crystal structure data, and starting coordinates for an asymmetric isomer of 3-Pd were obtained by rotation of the Se-bound methyl groups. No symmetry restrictions were applied. The nature of the stationary points as minima on the potential energy surfaces was confirmed by vibrational frequency calculations. Atomic charges were computed at the same level of theory as the geometry optimizations (ω B97X-D/def2-SVP) using natural population analysis as implemented in the program NBO6,³³ interfaced with the software package Gaussian09.³⁴ Kohn–Sham orbital isosurfaces were plotted at a contour level of 0.03 using wxMacMolPlt.³⁵ Details of converged structures are given in the Supporting Information.

RESULTS AND DISCUSSION

Ligand Synthesis. Our initial strategy followed the efforts of Ozerov and co-workers, who assembled a PNP diarylamido compound starting from di-*p*-tolylamine. Dibromination affords HN(2-Br-4-CH₃-C₆H₃)₂,¹⁹ which can undergo lithium-halogen exchange and N–H deprotonation with ⁿBuLi to afford the trilitio derivative [LiN((2-Li-4-CH₃-C₆H₃)₂)]. However, we found that reaction of this species with 2 equiv of Ph₂Se₂ or PhSeCl did not result in clean C–Se bond formation. Intractable mixtures were obtained using a variety of reaction conditions (e.g., different organolithium reagents, temperatures, solvents). In order to minimize chances of unwanted reactivity at the nitrogen center, the dibromo compound was deprotonated using [NaN(SiMe₃)₂] and protected as N–Me or N–Boc derivatives using MeI and Boc₂O, respectively. The Boc group was selected as a protecting group as it is stable to ⁿBuLi yet can be easily cleaved at a later stage by trifluoroacetic acid to regenerate the N–H functional group. These compounds, when dilithiated, also failed to yield the desired products upon reaction with the chosen selenium electrophiles. Another strategy was pursued, involving Buchwald–Hartwig cross-coupling^{36,37} of 2-phenylselenylaniline³⁸ with 1-bromo-2-(phenylselenyl)benzene,³⁹ in a process similar to that used by Peters and co-workers to generate a SNS diarylamido pincer ligand.¹⁰ Unfortunately, the cross-coupling approach also failed to produce our target molecule, with several Pd sources and ligands, and a variety of reaction conditions.

Turning our attention to differently substituted selenium electrophiles, we were gratified to observe that Me₂Se₂ reacted with dilithio Me- or Boc-protected species to generate methylselenenyl-containing compounds 1 and 2, respectively, as solids in 25–27% yield after recrystallization (Scheme 1). Though less electrophilic than Ph₂Se₂, the Me₂Se₂ is perhaps less likely to undergo undesired redox side reactions (in reactions with PhSeCl, a commonly observed byproduct was the reduction product Ph₂Se₂). The Boc-substituted compound 2 was readily deprotected with trifluoroacetic acid in dichloromethane to afford the protio ligand 3-H as an oil, in near-quantitative yield. The compounds 1, 2, and 3-H are all air-stable, and 3-H can be subject to silica gel column chromatography without decomposition, unlike alkylphosphine-containing analogues, which are sensitive to oxidation in air.

¹H, ¹³C, and ⁷⁷Se NMR spectroscopy unambiguously established the presence of the selenium donor group, –SeCH₃,

Scheme 1. Synthetic Route to Pincer Ligands **1**, **2**, and **3-H**^a

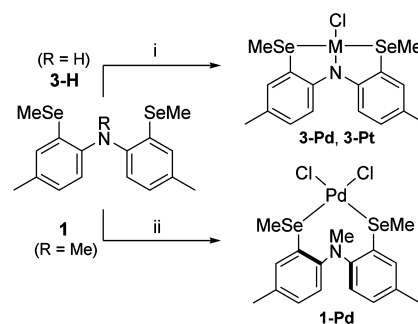
^aReaction conditions: (a) (1) $[\text{NaN}(\text{SiMe}_3)_2]$, toluene, 4 h, RT; (2) Boc_2O or MeI , THF, 27 h, RT. (b) (1) $2 \text{ }^t\text{BuLi}$, Et_2O , 2 h, $-78 \text{ }^\circ\text{C}$ to RT; (2) $2 \text{ Me}_2\text{Se}_2$, Et_2O , 27 h, $-78 \text{ }^\circ\text{C}$ to RT. (c) $\text{F}_3\text{CCO}_2\text{H}$, CH_2Cl_2 , 1 h, RT.

in compounds **1**, **2**, and **3-H**. New singlet resonances in the ^1H NMR spectra at δ 2.24 (**1**), 2.35 (**2**), and 2.29 (**3-H**) ppm indicate the additional methyl environment, which was corroborated by new ^{13}C signals at δ 5.8 (**1**), 7.7 (**2**), and 7.4 (**3-H**) ppm regions. ^{77}Se satellites are observed in the ^1H NMR spectra with coupling constants $^2J_{\text{H-Se}} = 12 \text{ Hz}$ consistent with the dimethyl diselenide coupling constant $^2J_{\text{H-Se}} = 12 \text{ Hz}$.⁴⁰ The ^{77}Se resonances of δ 178 (**1**), 179–173 (**2**), and 120 (**3-H**) are consistent with mixed alkyl/aryl selenides, e.g., *o*-tolyl methyl selenide resonates at δ 162.⁴¹

The NMR spectra of Boc-protected compound **2** indicated the presence of atropisomers in solution, as evidenced by two ^{77}Se signals at δ 173 and 179 and broadened signals in the ^1H spectrum corresponding to the tolyl group. This is likely due to restricted rotation of the large *t*-butoxycarbonyl group about the carbamate C–N bond, rendering the methylselenyl groups chemically inequivalent; the smaller methyl compound **1** does not exhibit this atropisomerism.

Group 10 Coordination Chemistry. The methyl-protected ligand **1** was reacted directly with $[\text{PdCl}_2(\text{COD})]$ in toluene at $100 \text{ }^\circ\text{C}$. It was hypothesized that the reaction would result in the metal cleaving the N–Me bond to form **3-Pd** and MeCl , as reported by Ozerov and co-workers for related PNP and NNN ligands.^{42,43} The N–Me bond, however, remained intact, and a bidentate complex, $[(\text{Se},\text{Se})\text{PdCl}_2]$ (**1-Pd**), resulted. The product was recrystallized from dichloromethane/ether as orange crystals in 57.8% yield. N–C cleavage reactivity at palladium has been reported where strong σ -donor groups such as mesitylimino or diisopropylphosphino are present, but not for groups such as diphenylphosphino.²⁰ Presumably, the methylseleno groups do not donate sufficient electron density to the metal to favor oxidative addition under the conditions investigated (*vide infra* for computational studies).

Anionic pincer ligand formation from **3-H** was achieved using $[\text{MCl}_2(\text{COD})]$ ($\text{M} = \text{Pd}, \text{Pt}$) reagents (Scheme 2). The addition of triethylamine to a mixture of $[\text{PdCl}_2(\text{COD})]$ and **3-H** resulted in an immediate color change from yellow to emerald green. The reaction was heated for 1 h to drive it to completion. The desired product was recrystallized from layered dichloromethane and diethyl ether at $-35 \text{ }^\circ\text{C}$ to afford 58.0% yield of product. The platinum species was prepared in a similar manner to afford a red powder and was recrystallized from layered dichloromethane and diethyl ether at $-35 \text{ }^\circ\text{C}$ to give an 87.9% yield. The stability of **3-Pt** is notable; it has been purified by silica gel column chromatography without

Scheme 2. Synthesis of Group 10 Metal Complexes of Ligands^a

^aConditions: (i) $[\text{MCl}_2(\text{COD})]$, NEt_3 , THF, 1 h, $80 \text{ }^\circ\text{C}$. (ii) $[\text{PdCl}_2(\text{COD})]$, toluene, 2 h, $100 \text{ }^\circ\text{C}$.

significant decomposition. Attempts to form **3-M** ($\text{M} = \text{Ni}, \text{Ir}, \text{Rh}$) were unsuccessful using various conditions and metal precursors ($[\text{NiCl}_2]$, $[\text{NiCl}_2(\text{DME})]$, $[\text{NiCl}_2(\text{H}_2\text{O})_6]$, $[\text{NiBr}_2]$, $[\text{Ni}(\text{OTf})_2]$, $[\text{Ir}_2(\text{C}_8\text{H}_{14})_4\text{Cl}_2]$, and $[\text{Rh}_2(\text{C}_8\text{H}_{14})_4\text{Cl}_2]$). Further efforts toward synthesis of these complexes are in progress.

Each new complex has been characterized by ^1H , ^{13}C , and ^{77}Se NMR. The ^1H NMR spectra of **3-Pd** displayed two singlets at δ 2.74 and 2.72 with ^{77}Se satellites ($^2J_{\text{H-Se}} = 12 \text{ Hz}$). This is indicative of two isomers with respect to the metal center, as would be expected for two selenium donor centers that become chiral upon coordination. The ^{13}C NMR spectrum indicated three methyl environments and six unique aryl resonances in the 115–155 ppm region. The ^{77}Se NMR spectrum indicated two distinct resonances at δ 305 and 298, again consistent with two isomers present in solution. The platinum complex experiences a similar bonding environment with two isomeric forms in solution. ^{195}Pt satellites were observed in the ^{77}Se spectrum of **3-Pt** with coupling constants ($^1J_{\text{Se-Pt}} = 439, 456 \text{ Hz}$) consistent with that observed for $[\text{PtCl}_2(\text{SeMe}_2)_2]$ ($^1J_{\text{Se-Pt}} = 480 \text{ Hz}$).⁴⁴ The ^{77}Se NMR chemical shifts are sensitive to the nature of M , and in accordance with increased shielding from platinum versus palladium, **3-Pt** resonates at ca. 40 ppm upfield of **3-Pd**, consistent with trends in the ^{31}P chemical shifts for PNP analogues.⁴⁵

X-ray Crystallography. Suitable quality single crystals of **1**, **1-Pd**, and **3-M** ($\text{M} = \text{Pd}, \text{Pt}$) have been obtained and their structures analyzed by X-ray crystallography. The structure of **1** served to confirm the structure of the methyl-protected ligand and contained no exceptional features. The metal complexes were identified as monometallic complexes featuring coordination by the methylselenyl groups. Thermal ellipsoid plots of metal complexes **1-Pd** and **3-Pd** (**3-Pt** is isostructural) are shown in Figures 2 and 3 along with selected bond lengths and angles. The geometry around the metal centers in complex **1-Pd** is approximately square-planar (sum of angles of 360.4° ; angles between *cis*-groups $83.6\text{--}93.8^\circ$). The C_2 -symmetric complexes **3-M** ($\text{M} = \text{Pd}, \text{Pt}$) are perfectly planar around the metal with *cis* angles ranging from 86.0 to 94.0° . The angular deviations from ideal square planar geometries are smaller than those of the analogous PNP–Pd complex (81.77°),⁴⁶ while larger than those of an NNN–Pd complex ($89.36\text{--}90.52^\circ$).⁴² While there are numerous examples of chalcogen-containing bimetallic complexes of Pd(II) and Pt(II) featuring bridging chloride ligands, a search of the Cambridge Structural Database revealed that these **3-Pd** and **3-Pt** are the first structurally

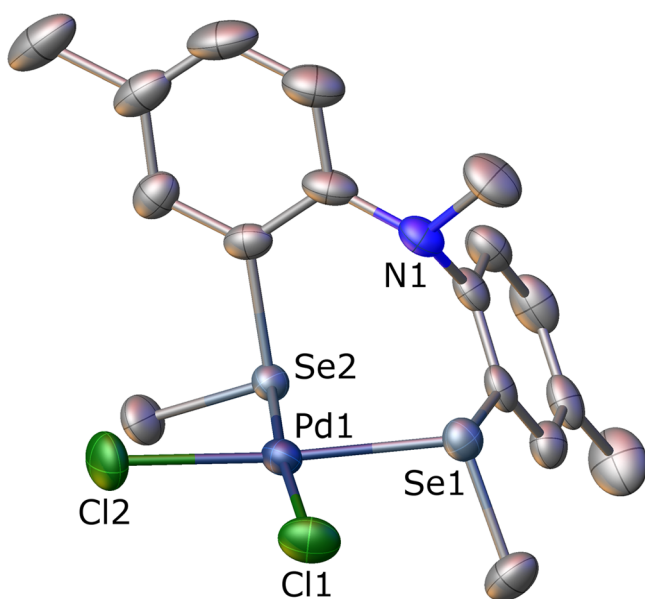


Figure 2. Thermal ellipsoid plot (50% probability) of **1-Pd**. Hydrogen atoms are omitted for clarity. Selected bond distances (Å) and angles (deg): Pd1–Se1, 2.4095(5); Pd1–Se2, 2.3944(5); Pd1–Cl1, 2.3424(11); Pd1–Cl2, 2.3247(12); Se1–Pd1–Se, 2 91.443(18); Cl1–Pd1–Se1, 83.57(3); Cl2–Pd1–Se2, 91.67(3); Cl1–Pd1–Cl2, 93.75(4).

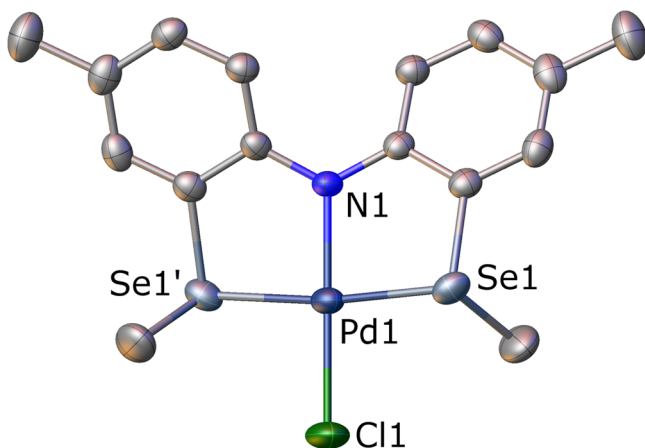


Figure 3. Thermal ellipsoid plot (50% probability ellipsoids) of **3-Pd**. Hydrogen atoms are omitted for clarity. Symmetry-equivalent positions (marked by ') are generated by C_2 rotation; the axis is coincident with the collinear N1–Pd1–Cl1 fragment. Selected bond distances (Å) and angles (deg): Pd1–Se1, 2.3841(4); Pd1–N1, 1.999(4); Pd1–Cl1, 2.3077(15); Se1–Pd1–Se1', 172.42(2); Cl1–Pd1–Se1, 93.788(12); N1–Pd1–Se1, 86.212(12).

characterized neutral, monomeric complexes with the coordination environment $[MSe_2NCl]$ ($M = Pd, Pt$).

The ligands **1** and **3** are coordinated with palladium(II) via bidentate SeSe and tridentate SeNSe modes, respectively. The Pd–Se bond lengths of complex **1-Pd** are 2.3944(5) Å and 2.4095(5) Å, while for **3-Pd** they are slightly shorter at 2.3841(4) Å. These values are consistent with reported values of bidentate ligands (2.3575(3) Å for $[PdCl_2\{o-NH_2(SePh)C_6H_4\}]$;⁴⁷ 2.3806(7) Å for $[PdCl_2\{1-PhSe-2-(4-Br-C_3H_3N_2)C_2H_4\}]$;⁴⁸) and tridentate ligands (2.370(1) Å for $[PdCl\{2-O-3,5-(C(CH_3)_3)_2-C_6H_2-C\equiv N-(CH_2)_2SePh\}]$;⁴⁹ 2.3910(13) Å for $Na[PdCl\{2,6-(CH_2(SePh))_2-C_5H_3N\}][PdCl_4]$).¹⁵ The Pd–N

bond length of **3-Pd** is 1.999(4) Å, which is very similar to the value of 2.035(3) Å for $[PdCl_2\{1-PhSe-2-(4-Br-C_3H_3N_2)C_2H_4\}]$;⁴⁸ and within experimental error of the distance of 1.996(4) Å for $[PdCl\{2-O-3,5-(C(CH_3)_3)_2-C_6H_2-C\equiv N-(CH_2)_2SePh\}]$.⁴⁹

The structure of **3-Pd** features a single isomer and does not exhibit disorder, and thus it is not consistent with the solution NMR data, which indicates two isomers with respect to the relative orientations of the –SeMe groups. There is no clear preference for one isomer over another in solution (*vide infra* for DFT energy calculations), while a single isomer preferentially crystallized out of solution. Each aryl group of the ligand is twisted out of plane relative to the other in the same molecule in **1**, **1-Pd**, and **3-Pd** (twist angles of 87.77(2)°, 96.48(15)°, and 39.80(15)°, respectively). The closest intermolecular Se⋯Cl distances in **1-Pd** and **3-Pd** are 4.2438(12) Å and 4.1486(4) Å, which lie outside the sum of the van der Waals radii (3.65 Å),⁵⁰ and there is no evident hydrogen bonding. The aryl groups are associated with the same group on an adjacent molecule by a slipped π stacking interaction in **3-Pd**. The centroid-to-centroid separation of aromatic rings is 3.724(3) Å, while the nearest centroid to plane distance is 3.427(3) Å. Together, these are indicative of the slipped nature of the weak π – π interaction (average interplanar distance 3.3–3.8 Å).⁵¹

The platinum(II) complex **3-Pt** is isostructural with **3-Pd** and hence possesses the same general features as the palladium complex. The M–Se bond lengths differ slightly (the platinum–selenium distance is contracted by <1%), and all other distances in the square plane are equal within experimental error. The π – π stacking is slightly closer in the platinum complex (centroid–centroid separation of 3.664(3) Å; nearest centroid–plane separation of 3.382(3) Å), accounting for the *ca.* 2% smaller volume of the **3-Pt** unit cell versus **3-Pd**.

Computational Chemistry. DFT calculations (ω B97X-D/def2-SVP) demonstrated a negligible energy difference ($\Delta G^\circ \approx 2$ kJ mol^{−1}) between the experimentally observed C_2 -symmetric Pd complex **3-Pd** and an asymmetric isomer with both Se-bound Me groups oriented on the same side of the square plane. This is consistent with one isomer preferentially crystallizing in the solid state, while in solution the two isomers are present in equal amounts—in keeping with the observed NMR spectral data for **3-Pd** and **3-Pt**.

To study the effect of the pincer ligand **D** on the resultant complexes **3-Pd** and **3-Pt**, these compounds were examined using DFT at the ω B97X-D/def2-SVP level of theory. The converged geometries matched well with experimental crystal structure data; the bond distances within the square-planar ML_4 moiety agreed within 1–2%. In order to compare the donor properties of **D** versus an analogous putative phosphine ligand, $[N(C_7H_6(PMe_2))_2]^-$ (**E**), structures were calculated for structures where the –SeMe groups were replaced by –PMe₂; **E-Pd** and **E-Pt**. The frontier orbitals of these four structures are illustrated in Figure 4. The HOMOs of all four complexes are similar, largely featuring ligand N(p) and aryl C(p) character, and having no significant contribution from the Se or P atoms. Thus, one-electron oxidation of these systems is predicted to involve primarily ligand-centered electron density, as has been concluded by Ozerov et al. for a series of PNZ ($Z = P$ or N) ligands based on $E_{1/2}$ values from cyclic voltammetry experiments.⁴³ The selenium-containing complexes feature HOMO energies that are *ca.* 0.2 eV lower and hence are predicted to exhibit higher oxidation potentials than the phosphine-bearing complexes.

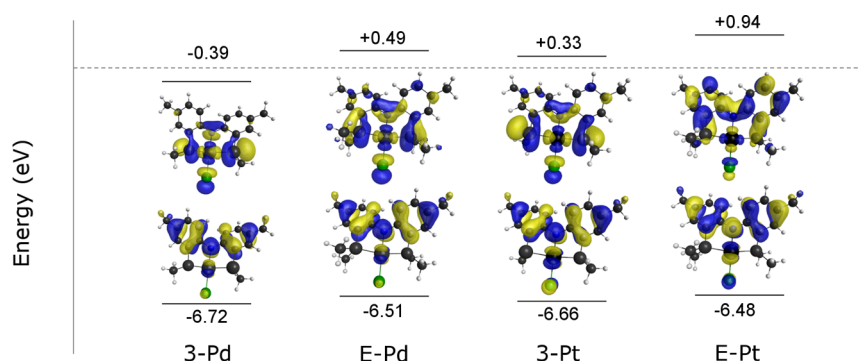


Figure 4. Calculated HOMO and LUMO orbitals for complexes of **D** and **E**.

The LUMOs feature significant contributions from the Se or P atoms and are quite different in energy depending on the donor atom, as reflected in the HOMO–LUMO gaps (3-Pd, 6.33 eV; E-Pd, 6.98 eV; 3-Pt, 7.00 eV; E-Pt, 7.41 eV). The lower HOMO–LUMO gaps for the Se compounds are consistent with ligand **D** being a weaker σ donor than **E**, as the LUMO is σ -antibonding with respect to the ML_4 plane, while the HOMO is σ nonbonding.

Computed natural charges of the five square-planar atoms for these complexes are shown in Table 1. For all complexes, the

Table 1. Computed Atomic Charges Using Natural Population Analysis

	3-Pd	E-Pd	3-Pt	E-Pt
M	+0.43	+0.36	+0.36	+0.30
Cl	−0.56	−0.55	−0.54	−0.53
N	−0.67	−0.67	−0.67	−0.67
E ^a	+0.56	+0.99	+0.59	+1.01

^aThe near-identical values for pairs of E = Se or P atoms are averaged.

natural charges on nitrogen and chlorine are very consistent. In keeping with the higher electronegativity of selenium versus phosphorus, the charges for selenium atoms are in the range +0.56–0.59, while for phosphorus they are ca. +1.00. The metal charges are concomitantly higher for the selenium-containing complexes, which is also consistent with less σ -donation from selenium to metal compared to the phosphine complexes. An inverse correlation between electron-donating ability and oxidation potential has been previously observed.⁴³

CONCLUSIONS

Several new organoselenium compounds have been prepared via a lithium-halogen exchange strategy, en route to the successful synthesis of a new selenium-containing anionic [SeNSe][−] pincer ligand, **D**. This ligand has been coordinated to palladium(II) and platinum(II) to generate heteroleptic complexes of potential relevance to homogeneous catalysis and materials chemistry. Computational studies comparing 3-M (M = Pd, Pt) to phosphine analogues indicate that the σ -donor ability of the ligand **D**, and the frontier orbitals (particularly the LUMO levels) of the resultant complexes are significantly different, indicating that the reactive chemistry of these selenium-bearing ligands may prove unique. Synthesis of complexes of other metals, and organometallic derivatives of 3-M (M = Pd, Pt), as well as an assessment of their suitability to catalyze coupling reactions will be the subject of a future contribution.

ASSOCIATED CONTENT

Supporting Information

The Supporting Information is available free of charge on the ACS Publications website at DOI: 10.1021/acs.inorgchem.6b01203.

Experimental conditions for Ni(II) reactions, selected crystal data, and atomic coordinates and energies for DFT geometry optimizations (PDF)

Crystallographic data in CIF format for compounds **1**, **1-Pd**, **3-Pd**, and **3-Pt** (CIF)

AUTHOR INFORMATION

Corresponding Author

*email: j.ritch@uwinnipeg.ca ph: +1-204-786-9730 fax: +1-204-774-2401.

Notes

The authors declare no competing financial interest.

ACKNOWLEDGMENTS

Funding from The University of Winnipeg and the Province of Manitoba (Career Focus Program) is gratefully acknowledged. We thank Dr. David Herbert (University of Manitoba) for access to a single-crystal X-ray diffractometer and Mr. Xiao Feng for mass spectrometric analysis of compound **3-H**. The Department of Chemistry, University of Manitoba is thanked for an adjunct appointment. Dr. Joshua Hollett (The University of Winnipeg) is thanked for useful discussions regarding DFT calculations.

REFERENCES

- Chase, P. A.; Gossage, R. A.; van Koten, G. In *The Privileged Pincer-Metal Platform: Coordination Chemistry & Applications*; van Koten, G., Gossage, R. A., Eds.; Topics in Organometallic Chemistry; Springer International Publishing, 2015; pp 1–15.
- McGowan, K. P.; O'Reilly, M. E.; Ghiviriga, I.; Abboud, K. A.; Veige, A. S. *Chem. Sci.* **2013**, *4*, 1145–1155.
- Gao, W.; Cui, D. *J. Am. Chem. Soc.* **2008**, *130*, 4984–4991.
- Scheuermann, M. L.; Semproni, S. P.; Pappas, I.; Chirik, P. J. *Inorg. Chem.* **2014**, *53*, 9463–9465.
- Bleith, T.; Wadepohl, H.; Gade, L. H. *J. Am. Chem. Soc.* **2015**, *137*, 2456–2459.
- Melnick, J. G.; Radosevich, A. T.; Villagrán, D.; Nocera, D. G. *Chem. Commun.* **2010**, *46*, 79–81.
- Choi, J.; MacArthur, A. H. R.; Brookhart, M.; Goldman, A. S. *Chem. Rev.* **2011**, *111*, 1761–1779.
- Bézier, D.; Guan, C.; Krogh-Jespersen, K.; Goldman, A. S.; Brookhart, M. *Chem. Sci.* **2016**, *7*, 2579–2586.
- Errington, J.; McDonald, W. S.; Shaw, B. L. *J. Chem. Soc., Dalton Trans.* **1980**, *11*, 2312–2314.

- (10) Harkins, S. B.; Peters, J. C. *J. Am. Chem. Soc.* **2004**, *126*, 2885–2893.
- (11) Albahily, K.; Gambarotta, S.; Duchateau, R. *Organometallics* **2011**, *30*, 4655–4664.
- (12) Spasyuk, D.; Smith, S.; Gusev, D. G. *Angew. Chem., Int. Ed.* **2013**, *52*, 2538–2542.
- (13) Locke, H.; Herrera, A.; Heinemann, F. W.; Linden, A.; Frieß, S.; Schmid, B.; Dorta, R. *Organometallics* **2015**, *34*, 1925–1931.
- (14) Yao, Q.; Kinney, E. P.; Zheng, C. *Org. Lett.* **2004**, *6*, 2997–2999.
- (15) Das, D.; Rao, G. K.; Singh, A. K. *Organometallics* **2009**, *28*, 6054–6058.
- (16) Kumar, S.; Rao, G. K.; Kumar, A.; Singh, M. P.; Singh, A. K. *Dalton Trans.* **2013**, *42*, 16939–16948.
- (17) Kumar, A.; Rao, G. K.; Saleem, F.; Singh, A. K. *Dalton Trans.* **2012**, *41*, 11949–11977.
- (18) Kumar, A.; Rao, G. K.; Kumar, S.; Singh, A. K. *Organometallics* **2014**, *33*, 2921–2943.
- (19) Fan, L.; Yang, L.; Guo, C.; Foxman, B. M.; Ozerov, O. V. *Organometallics* **2004**, *23*, 4778–4787.
- (20) Fan, L.; Yang, L.; Guo, C.; Foxman, B. M.; Ozerov, O. V. *Organometallics* **2004**, *23*, 4778–4787.
- (21) Clark, D. L.; Sattelberger, A. P.; Andersen, R. A. In *Inorganic Syntheses*; Cowley, A. H., Ed.; John Wiley & Sons, Inc., 1996; pp 307–315.
- (22) Drew, D.; Doyle, R.; Shaver, A. G. *Inorg. Synth. Reag. Transit. Met. Complex Organomet. Synth.* Angelici, R. J., Ed.; 1990, *28*, pp 346–349.
- (23) Tronnier, A.; Poethig, A.; Herdtweck, E.; Strassner, T. *Organometallics* **2014**, *33*, 898–908.
- (24) Boudier, A.; Breuil, P.-A. R.; Magna, L.; Olivier-Bourbigou, H.; Braunstein, P. *J. Organomet. Chem.* **2012**, *718*, 31–37.
- (25) Ozerov, O. V.; Guo, C.; Papkov, V. A.; Foxman, B. M. *J. Am. Chem. Soc.* **2004**, *126*, 4792–4793.
- (26) Dolomanov, O. V.; Bourhis, L. J.; Gildea, R. J.; Howard, J. A. K.; Puschmann, H. *J. Appl. Crystallogr.* **2009**, *42*, 339–341.
- (27) Sheldrick, G. M. *Acta Crystallogr., Sect. A: Found. Adv.* **2015**, *71*, 3–8.
- (28) Sheldrick, G. M. *Acta Crystallogr., Sect. A: Found. Crystallogr.* **2008**, *64*, 112–122.
- (29) Schmidt, M. W.; Baldrige, K. K.; Boatz, J. A.; Elbert, S. T.; Gordon, M. S.; Jensen, J. H.; Koseki, S.; Matsunaga, N.; Nguyen, K. A.; Su, S.; Windus, T. L.; Dupuis, M.; Montgomery, J. A. *J. Comput. Chem.* **1993**, *14*, 1347–1363.
- (30) Chai, J.-D.; Head-Gordon, M. *Phys. Chem. Chem. Phys.* **2008**, *10*, 6615–6620.
- (31) Minenkov, Y.; Singstad, Å.; Occhipinti, G.; Jensen, V. R. *Dalton Trans.* **2012**, *41*, 5526–5541.
- (32) Weigend, F.; Ahlrichs, R. *Phys. Chem. Chem. Phys.* **2005**, *7*, 3297–3305.
- (33) Glendening, E. D.; Badenhoop, J. K.; Reed, A. E.; Carpenter, J. E.; Bohmann, J. A.; Morales, C. M.; Landis, C. R.; Weinhold, F. *NBO 6.0*; Theoretical Chemistry Institute, University of Wisconsin: Madison, WI, 2013.
- (34) Frisch, M. J.; Trucks, G. W.; Cheeseman, J. R.; Scalmani, G.; Caricato, M.; Hratchian, H. P.; Li, X.; Barone, V.; Bloino, J.; Zheng, G.; Vreven, T.; Montgomery, J. A.; Petersson, G. A.; Scuseria, G. E.; Schlegel, H. B.; Nakatsuji, H.; Izmaylov, A. F.; Martin, R. L.; Sonnenberg, J. L.; Peralta, J. E.; Heyd, J. J.; Brothers, E.; Ogliaro, F.; Bearpark, M.; Robb, M. A.; Mennucci, B.; Kudin, K. N.; Staroverov, V. N.; Kobayashi, R.; Normand, J.; Rendell, A.; Gomperts, R.; Zakrzewski, V. G.; Hada, M.; Ehara, M.; Toyota, K.; Fukuda, R.; Hasegawa, J.; Ishida, M.; Nakajima, T.; Honda, Y.; Kitao, O.; Nakai, H. *Gaussian 09*; Gaussian, Inc.: Wallingford, CT, 2013.
- (35) Bode, B. M.; Gordon, M. S. *J. Mol. Graphics Modell.* **1998**, *16*, 133–138.
- (36) Surry, D. S.; Buchwald, S. L. *Chem. Sci.* **2011**, *2*, 27–50.
- (37) Fors, B. P.; Watson, D. A.; Biscoe, M. R.; Buchwald, S. L. *J. Am. Chem. Soc.* **2008**, *130*, 13552–13554.
- (38) Deobald, A. M.; Simon de Camargo, L. R.; Tabarelli, G.; Hörner, M.; Rodrigues, O. E. D.; Alves, D.; Braga, A. L. *Tetrahedron Lett.* **2010**, *51*, 3364–3367.
- (39) Charette, B. J.; Ritch, J. S. *Acta Crystallogr. Sect. E Crystallogr. Commun.* **2015**, *71*, 327–329.
- (40) Lardon, M. *J. Am. Chem. Soc.* **1970**, *92*, 5063–5066.
- (41) McFarlane, W.; Wood, R. J. *J. Chem. Soc., Dalton Trans.* **1972**, *13*, 1397–1402.
- (42) Hollas, A. M.; Gu, W.; Bhuvanesh, N.; Ozerov, O. V. *Inorg. Chem.* **2011**, *50*, 3673–3679.
- (43) Davidson, J. J.; DeMott, J. C.; Douvris, C.; Fafard, C. M.; Bhuvanesh, N.; Chen, C.-H.; Herbert, D. E.; Lee, C.-I.; McCulloch, B. J.; Foxman, B. M.; Ozerov, O. V. *Inorg. Chem.* **2015**, *54*, 2916–2935.
- (44) McFarlane, W. *Chem. Commun.* **1968**, 755–756.
- (45) Ozerov, O. V.; Guo, C.; Fan, L.; Foxman, B. M. *Organometallics* **2004**, *23*, 5573–5580.
- (46) Fan, L.; Foxman, B. M.; Ozerov, O. V. *Organometallics* **2004**, *23*, 326–328.
- (47) Ritch, J. S.; Charette, B. J. *Can. J. Chem.* **2015**, *94*, 386–391.
- (48) Sharma, K. N.; Joshi, H.; Singh, V. V.; Singh, P.; Singh, A. K. *Dalton Trans.* **2013**, *42*, 3908–3918.
- (49) Kumar, U.; Dubey, P.; Singh, V. V.; Prakash, O.; Singh, A. K. *RSC Adv.* **2014**, *4*, 41659–41665.
- (50) Bondi, A. J. *Phys. Chem.* **1964**, *68*, 441–451.
- (51) Janiak, C. *J. Chem. Soc., Dalton Trans.* **2000**, No. 21, 3885–3896.10.1039/b003010o